Processing and analysis of data recorded from a buried permanent seismic source

Tyler W. Spackman and Don C. Lawton

ABSTRACT

The Containment and Monitoring Institute has established a Field Research Station in Newell County, Alberta for the purpose of testing various monitoring technologies in the context of carbon sequestration projects. This paper investigates the use of permanent seismic sources as a monitoring technique.

Installation and initial testing of permanent seismic sources at the Field Research Station was performed in September 2018. This study describes the differences between the permanent sources installed at the FRS, as well as the acquisition parameters used in the initial tests. We show the results of these initial tests, with a focus on the borehole source, and comment on some of the unique considerations for permanent source data. We also compare permanent source data to seismic data acquired with Vibroseis.

Raw, correlated permanent source data suffers from an extremely ringy character. We find that after applying Gabor deconvolution to the correlated data, the downgoing and upgoing wavefields are easily identifiable, and resultant images are comparable, if not superior to, those from a more conventional Vibroseis source.

INTRODUCTION

In Newell County, Alberta, approximately 200 kilometres southeast of Calgary, the Containment and Monitoring Institute (CaMI) has established a Field Research Station (FRS) to test various measurement, monitoring, and verification techniques on a small carbon sequestration project. At the FRS, small quantities of carbon dioxide are being injected into the Basal Belly River (BBR) formation at approximately 300 metres depth. The BBR at the FRS is approximately 10 metres thick and is comprised of shoreface sandstones overlain with low-density coal seams. It is anticipated that overlying mudstones and siltstone will serve as an adequate seal for the injection reservoir (Isaac and Lawton, 2014a).

A schematic of the FRS site is shown in Figure 1. The injection well, 10-22-017-16W4, is located approximately at the centre of the site, with the two observation wells, the “geophysics well”, containing distributed acoustic sensing (DAS) fibre and multicomponent geophones, and the “geochemistry well”, containing DAS fibre and fluid sampling ports, located approximately 20 metres southwest and 30 metres northeast, respectively, of the injector. Additionally, a shallow trench containing fibre optic and electrical resistivity tomography (ERT) cable runs approximately southwest to northeast through the site.

DATA ACQUISITION

Permanent seismic sources operate by rotating an eccentric, or unbalanced, mass in a circle about an axle that is fixed to the ground. As the mass rotates, it exerts a force on the

axle, which is then transferred to the ground, causing seismic waves to propagate through the subsurface. The mass rotates through a sweep of frequencies that is controlled by the user. The motion of the mass is easily modelled by sinusoidal functions of the sweep frequency and time. By reversing the rotation direction, or using two masses rotating in opposite directions, the horizontal component of particle motion can theoretically be cancelled out (Daley and Cox, 2001).

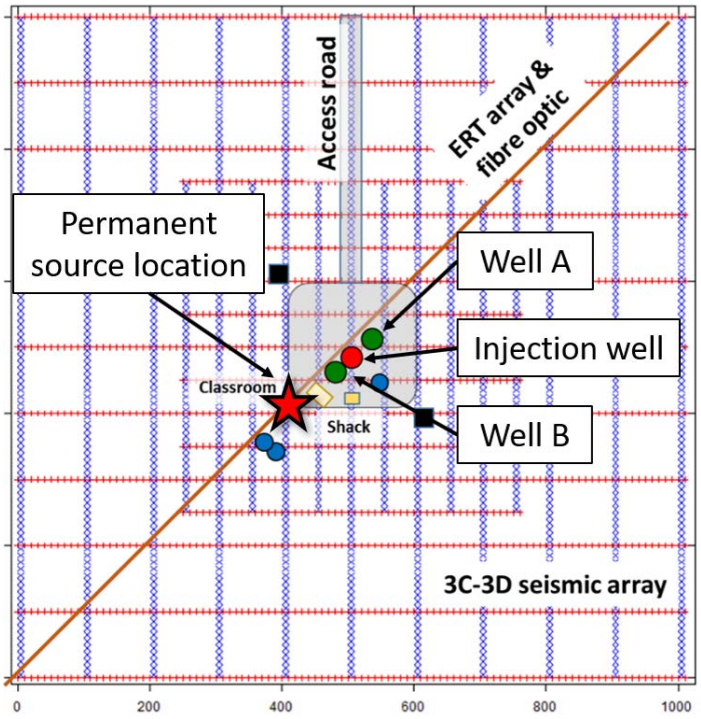

FIG. 1: Site schematic of the CaMI.FRS. The geochemistry well is Well A and the geophysics well is Well B.

Conceptually, permanent seismic sources are very similar to Vibroseis in the sense that each of these source types emit a sweep of frequencies into the subsurface, and that the recorded data must be correlated with a known source sweep signature before further analysis.

At the CaMI site, permanent sources were installed approximately 110 metres southwest of the geochemistry well, which is along an azimuth passing approximately through both the injection well and the geophysics well. This azimuth was chosen to best image the injected CO_2 plume using distributed acoustic sensing (DAS) fibre in the geochemistry well. As the chosen azimuth also passes through the geophysics well, future comparisons between DAS data from each of the wells will also be made. An offset of approximately 110 metres from the geochemistry well was chosen to maximize a combination of the illumination of the injected plume and the range of incidence angles recorded in the geochemistry well. These objectives were assessed through a simple raytracing experiment using the baseline FRS velocity model, which is derived from injector well logs (Spackman and Lawton, 2017).

Three permanent sources, all manufactured by GPUSA, were installed at the CaMI site (Table 1). A borehole source (Figure 2), with a horizontally oriented rotation axle, was installed and cemented in a well drilled in June 2018 to a depth of approximately 15 metres. Station 36, at the centre of the surface spread, was located immediately adjacent to the borehole, thus providing a rough estimate of the source signature. This trace could potentially be used to correlate the recorded data for each sweep.

In June 2018, a steel helical pile was installed to serve as a mount for permanent sources installed at the surface. The pile was drilled to a depth of approximately 15 metres where it is anchored to a hard-packed argillaceous layer below more poorly consolidated glacial till in the shallow near surface. The purpose of this pile is to transfer energy from the source to the anchor point at the end of the pile, thus allowing the source signature to bypass the attenuative near-surface layer. While the pile has not been anchored to the bedrock (which lies at a depth of approximately 30 metres), the consolidated argillaceous layer should be sufficient to transfer the source signature through the near surface layer.

FIG. 2: GPUSA borehole linear vibrator prior to installation.

Two permanent surface sources were installed and tested in early September 2018. Both of these sources were installed on the steel pile, and the base plate for each of the sources was bolted to a plate on the top of the pile. The first, and smaller, of the two surface sources tested was identical to the borehole source, with one horizontally oriented axle. Peak force exerted by this source was approximately 4,500 lbs., and the source is capable of sweeping up to a maximum frequency of approximately 200 Hz.

The second surface source tested, referred to as a surface linear vibrator (Figure 3), also had two horizontally-oriented rotation axles, which were connected by a timing belt. This

belt ensured that the eccentric counter-rotating masses inside the source remained in phase with each other. Peak force for this source was approximately 11,000 lbs., with maximum frequency approximately 100 Hz. During this phase of testing, the permanent sources were run as individual sweeps triggered manually on-site. Ideally, the sources would ultimately be able to be remotely operated and run semi-continuously; however more technical development is needed to progress to this stage.

Table 1: Permanent source parameters.

Source name	Frequency range (Hz)	Peak force (lbs.)
Downhole linear vibrator	0-200	4,500
Surface linear vibrator	0-200	4,500
Surface linear vibrator ("orange vibe")	0-100	11,000

FIG. 3: GPUSA surface linear vibrator mounted on baseplate, attached to helical pile.

The minimum frequency, maximum frequency, total sweep length, and time to sweep to each chosen frequency was specified prior to each sweep. However, despite these parameters being known, the sweep signature cannot be exactly modelled because the source was powered off once the maximum frequency was reached and allowed to come to rest naturally instead of in a controlled downsweep. Instead, the trace from the geophone closest to the source location was used for each sweep as the pilot trace to correlate the acquired data.

While it was intended that the steel pile transfer energy from the rotating sources to the anchor point, initial field tests indicate that this may not have occurred in practice. Video recordings of the surface vibrator show the pile vibrating, suggesting that instead of acting as a point source at the anchor point, the steel pile acts as a line source. Additionally, video shows the base plate of the source vibrating at low frequency, further compounding efforts to fully understand the source signature. These low-frequency vibrations could potentially

be explained by the fact that the helical pile on which the source was installed is not a single piece of metal; rather it is made of segments that are bolted together, allowing the segments to move slightly in the subsurface. The cumulative effects of the motion between segments may cause a low frequency overprint on the recorded data.

DOWNHOLE VIBRATOR DATA

In September 2018, the downhole linear vibrator, cemented into a shallow borehole, was tested with various sweep parameters. The vibrator tests were recorded with 24 3-component geophones installed in the geophysics well, approximately 58 metres away, and a spread of 24 single component geophones centred on the source location. The sweep parameters for the five sweeps analysed in this report are summarized in Table 2.

Table 2: Sweep parameters for downhole linear vibrator tests

Sweep number	Max frequency (Hz)	Upsweep/downsweep time (s)
1015	125	20
1017	200	25
1022	200	20
1024	200	20
1026	175	25

None of the five sweeps tested holding the vibrator frequency at the maximum frequency. In other words, after reaching the maximum frequency, the downsweep started immediately. Sweeps 1022 and 1024 were run with identical parameters. Unfortunately, the accelerometer mounted in the source failed and the geophone placed next to the borehole at the surface (station 36) had to be used as the pilot trace for correlation and further analysis. The traces from this station for each of the sweeps in Table 2 are shown in Figure 4.

In rotational kinematics, the centripetal acceleration a_c of an object rotating in a circle is given by the following equation:

$$a_c = r\omega^2 \tag{1}$$

where r is the radius of the rotating object's orbit and ω is the angular frequency. Therefore, the force exerted on the axle by the rotating eccentric mass in the linear vibrators, and, by Newton's Third Law of Motion, the force transferred to the ground, is also proportional to the square of the angular frequency. The amplitude spectra for each of the five pilot traces in Figure 4 are shown in Figure 5. The spectra show what appears to be a quadratic increase in amplitude up to the maximum frequency for each sweep, followed by an abrupt decrease in amplitude to approximately zero. The roll-off towards the maximum frequency is due to the anti-alias filter in the Geode recorders used for

acquisition. The amplitude spectra for the full surface spread for each of the five sweeps (Figure 6) is nearly identical to that of the pilot trace, exhibiting very similar changes in amplitude as frequency increases, as well as a sharp drop to nearly zero amplitude upon reaching the maximum frequency of the sweep.

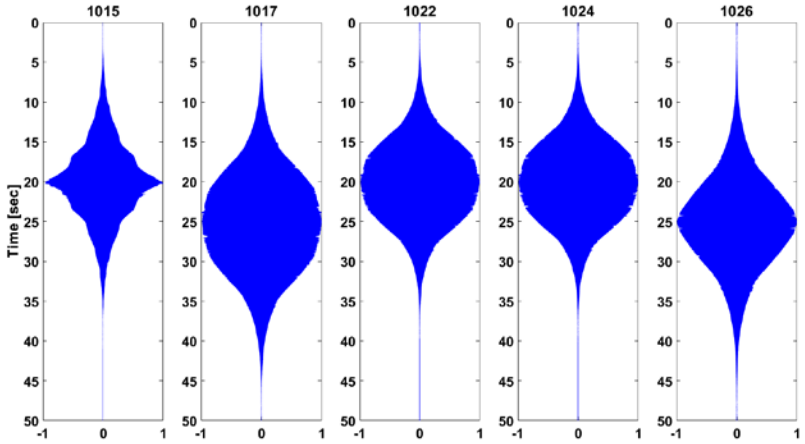

FIG. 4: Raw (uncorrelated) traces from geophone closest to GPUSA borehole linear vibrator location for five test sweeps.

Isolating the portion of the amplitude spectrum less than the maximum sweep frequency and fitting a quadratic curve confirms the dependence of amplitude on ω^2. Quadratic, exponential, and sinusoidal models were fit to the dominant frequency band of the amplitude spectrum. The quadratic models fit to the amplitude spectra exhibited the highest R^2 values of the model types tested, confirming the relationship between the observed amplitude and frequency (Table 3).

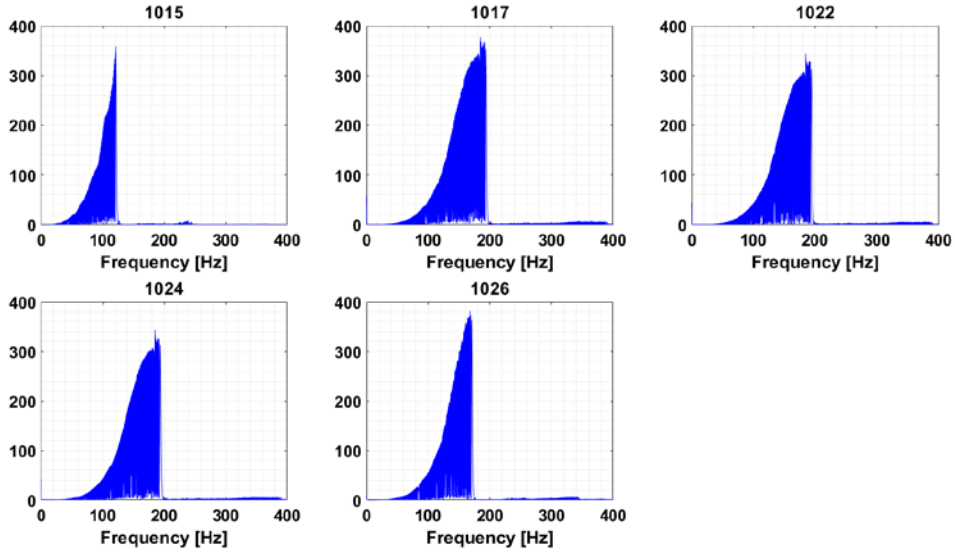

FIG. 5: Amplitude spectra of the pilot trace for each of the five GPUSA borehole linear vibrator test sweeps.

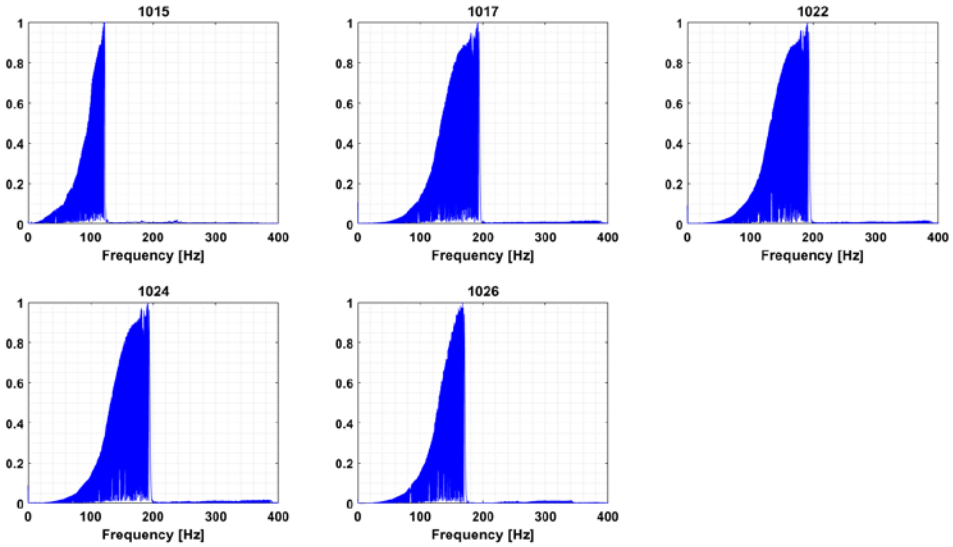

FIG. 6: Amplitude spectra of the surface spread for each of the five downhole source test sweeps.

Table 3: R^2 values for quadratic models fit to dominant frequency band of amplitude spectra for downhole linear vibrator tests

Sweep number	R^2 value
1015	0.6406
1017	0.5649
1022	0.5648
1024	0.5663
1026	0.6175

Computing the Gabor transform of the pilot traces and plotting the resultant time-frequency relationship yields extremely promising results (Figure 7). The Gabor transform for each sweep accurately reflects the sweep parameters listed in Table 2, with no visible energy outside of the dominant band. This implies that the sweep signature supplied to the vibrator is efficiently transferred to the subsurface, with little noticeable impact from the cement, borehole casing, or other sources of noise. The Gabor plots of the uncorrelated surface spread for each sweep (Figure 8) show a similar character to that of the plots for the pilot trace; however, some sources of noise have also been recorded. On each of the five plots, a high amplitude band is observed at all times at approximately 180 Hz. This is thought to be a 60 Hz harmonic.

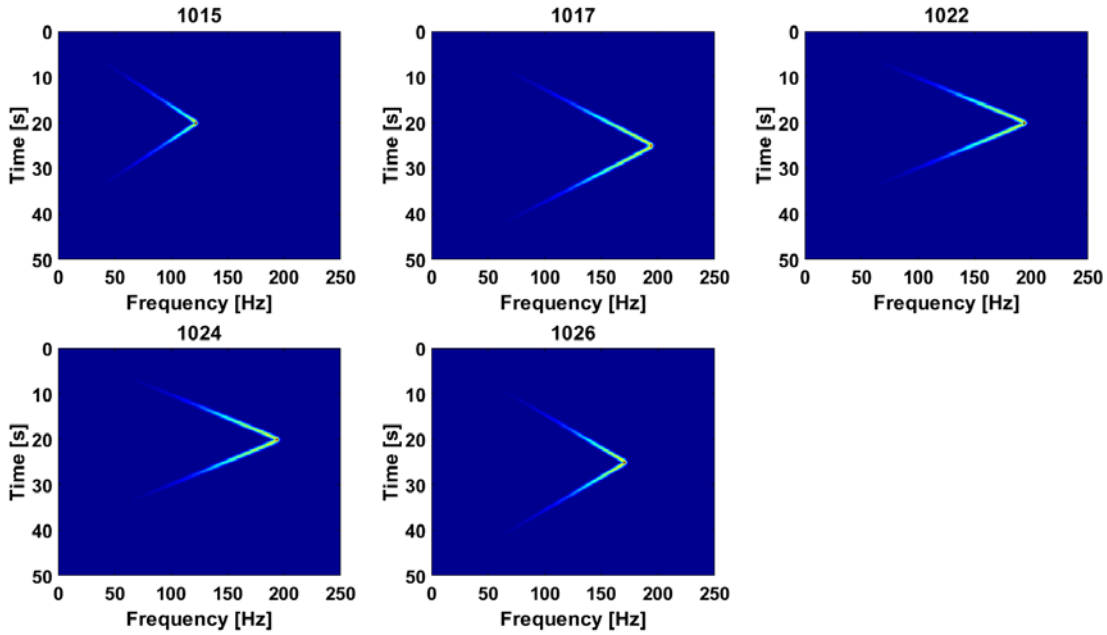

FIG. 7: Gabor transform plots of the pilot traces for each of the five downhole source test sweeps.

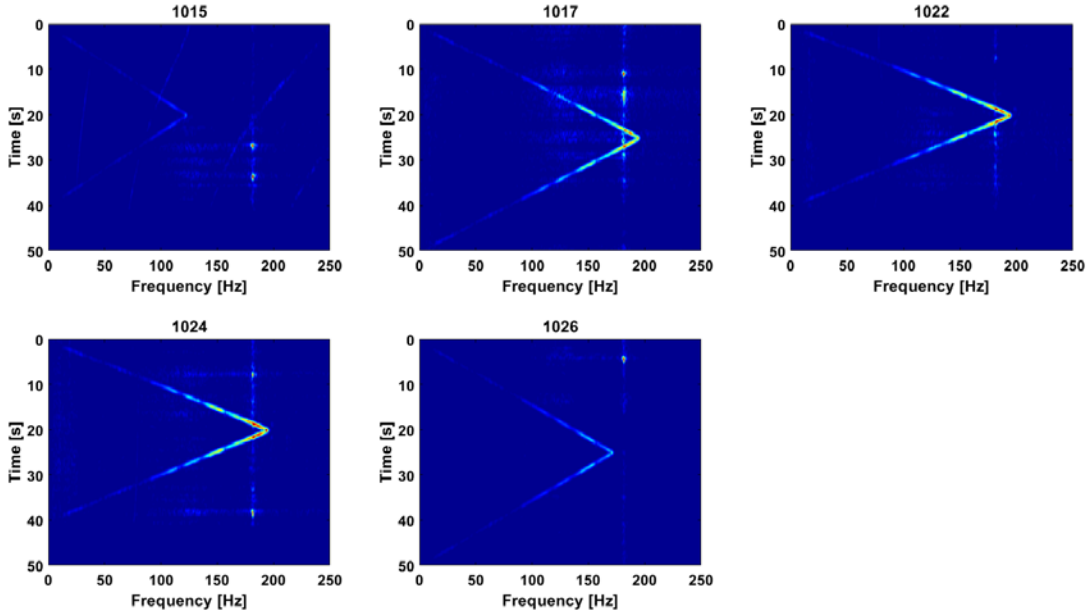

FIG. 8: Gabor transform plots of the surface spread for each of the five downhole source tests.

The signal recorded by the surface spread behaves much like that of the pilot trace, and indeed, like that of synthetic sweeps generated with known sweep parameters. The signature recorded by the geophones installed in the geophysics well is dominated by geophone harmonics at approximately 60 Hz and 180 Hz; however, the dominant band of the Gabor spectrum can be revealed by normalizing the response of each frequency (Figure 9). Although the plots are quite noisy, they do show that the source signature is being captured by the downhole geophones.

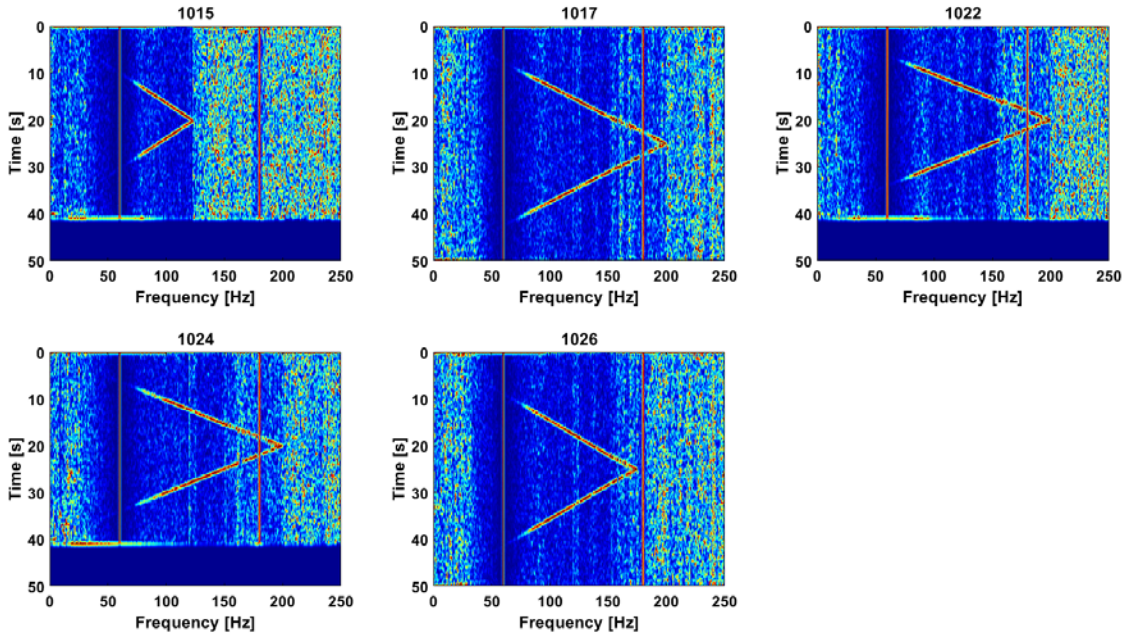

FIG. 9: Gabor transform plots of the downhole geophones for each of the five downhole source test sweeps.

Correlation

During typical Vibroseis acquisition, an accelerometer is used to understand the true motion of the baseplate. Similarly, permanent sources should ideally have an accelerometer mounted on the source to record the ground motion. This accelerometer trace could then be used to correlate the raw data. However, during the testing of the borehole linear vibrator, accelerometer failed and thus to create correlated sections, two options were tested:

1. Correlate with the geophone closest to the source location (i.e. a pilot trace); and,

2. Correlate with a synthetic sweep generated from the known sweep parameters.

Using the sweep parameters as listed in Table 2, synthetic sweep signatures were generated for each of the five permanent source test sweeps. The synthetic sweeps were scaled with a quadratic amplitude modifier, to satisfy the ω^2 relationship explained above, as well as a cosine taper. An example of these synthetic sweeps is shown in Figure 10. This figure shows that, while not an exact match, the quadratic-scaled trace more closely matches the raw trace than does the synthetic trace with a cosine taper.

The traces shown in Figure 10 were also used to correlate the raw data, and the best sections were used for further analysis. In the ideal case where the sweep signature transferred to the ground is known exactly, the autocorrelation of this sweep signature will collapse to a signal known as a Klauder wavelet. In the initial tests of the borehole linear vibrator, a geophone placed at the surface of the source borehole was used as a pilot trace for correlation. Therefore, if the synthetic sweep shown in Figure 10 is truly representative of the sweep signature, then the autocorrelation of the synthetic sweep should be similar to

that of the pilot trace. Additionally, the cross-correlation of the synthetic sweep and the pilot trace should also be a Klauder wavelet, with its maximum value at zero lag. However, computing this cross-correlation (Figure 11) indicates that this is not the case. Additionally, correlating both the synthetic sweep and the pilot trace with the raw VSP data yields significantly different results (Figures 12 and 13).

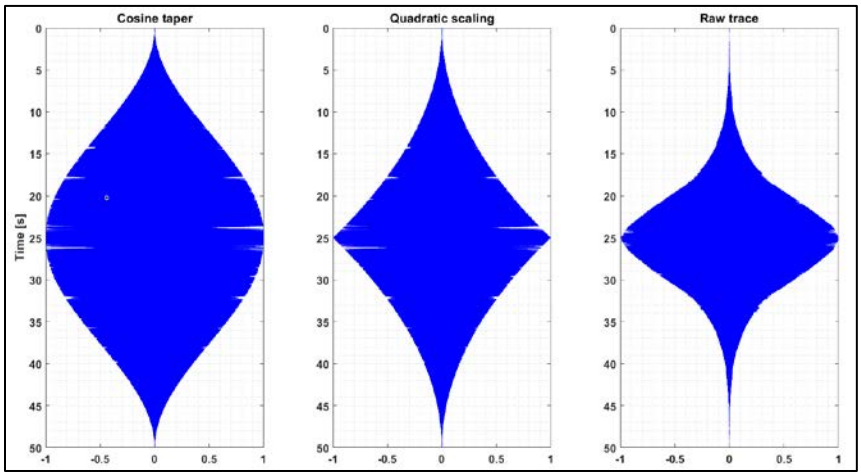

FIG. 10: Synthetic sweep examples for sweep parameters 0-175-0 Hz, 25 second upsweep and downsweep, 0 second hold time (i.e. sweep number 1026). Data shown: synthetic sweep with cosine taper (left); synthetic sweep with quadratic scaling (centre); and raw pilot trace (right).

Comparing the correlated data in Figures 12 and 13, it is evident that correlating the recorded VSP data with the synthetic sweep does not produce reliable results. Correlating with the pilot trace from surface station 36 produces an image with easily identifiable first break energy and is more representative of expected VSP data. If the synthetic sweep could be altered to more closely match the pilot trace, or accelerometer data from the borehole linear vibrator were available, more accurate correlated sections could be produced. This is currently being investigated.

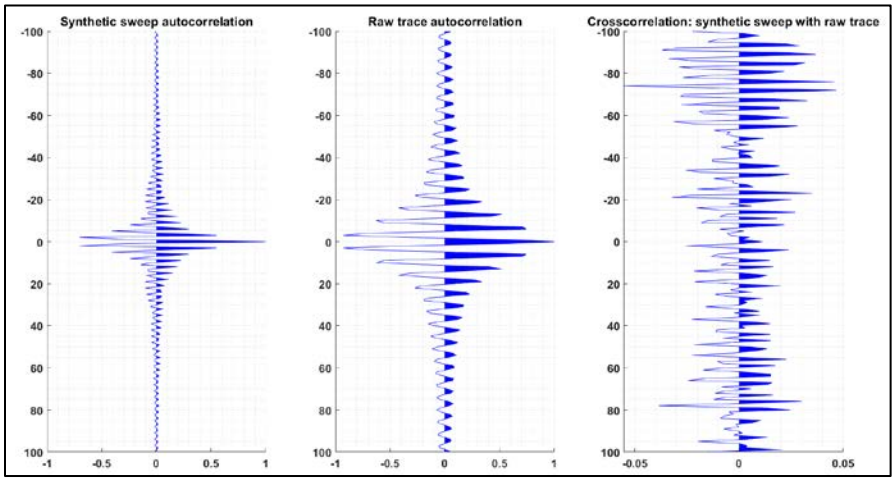

FIG. 11: Correlation tests for synthetic sweep and pilot trace. Quadratic-scaled synthetic sweep autocorrelation (left); raw pilot trace autocorrelation (centre); cross-correlation between synthetic sweep and pilot trace (right). Data shown is from sweep number 1026.

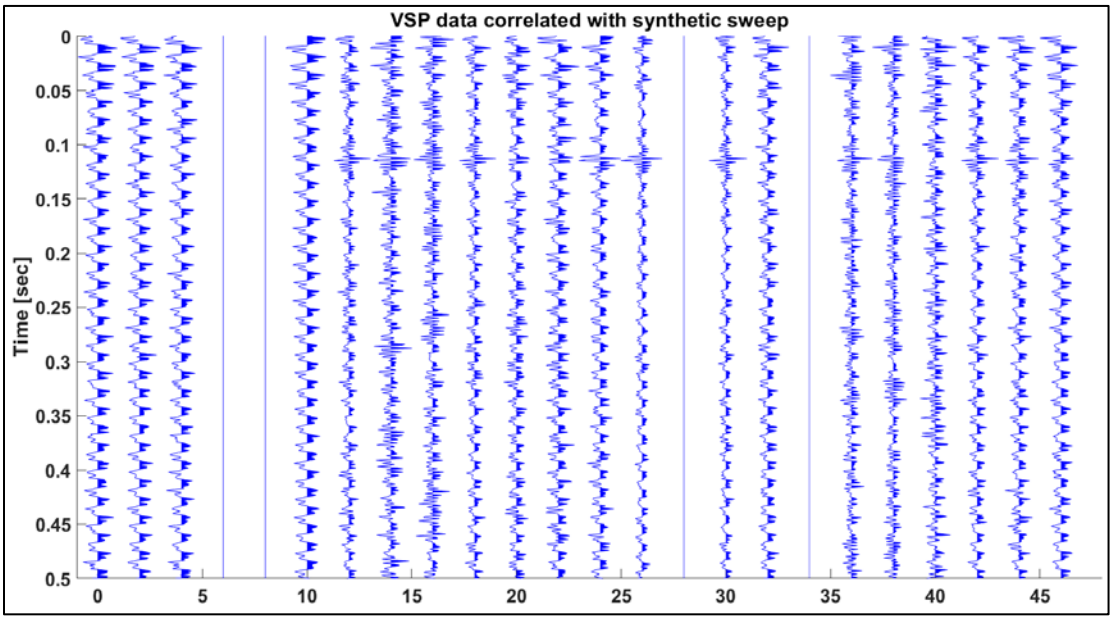

FIG. 12: VSP data correlated with synthetic sweep (with quadratic scaling). Dead traces have been killed and not interpolated. Data shown is from sweep number 1026.

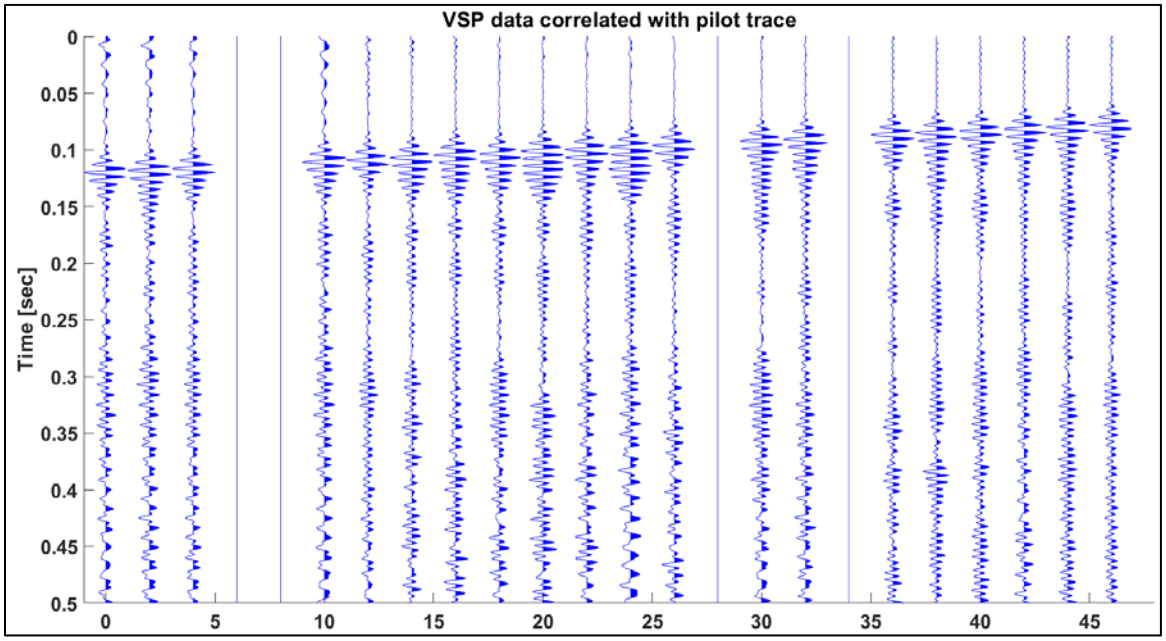

FIG. 13: VSP data correlated with pilot trace (surface station 36). Dead traces have been killed and not interpolated. Data shown is from sweep number 1026.

FIELD DATA

In September 2018, the GPUSA borehole linear vibrator was tested with various sweep parameters, using 24 multicomponent geophones in the geophysics well, and a small surface spread of single component geophones as the receivers. As discussed in the

previous section, correlated datasets were created by using the pilot trace, taken from the surface geophone at the surface of the source borehole, as an approximation of the source signature. An example of the correlated borehole linear vibrator data is shown in Figure 14.

For each of the tests, the same receiver geometry was used. Multicomponent geophones, with approximately a 5 m receiver interval in the geophysics well were used. The offset between the source borehole and the geophysics well is 58 metres. The source was cemented in the borehole at a depth of 15 metres. Surface geophones were installed at 10 metre intervals and centred on the source borehole. The remainder of this report will focus on VSP data from the geophones installed in the geophysics well.

An example of the VSP data from one of the vibrator tests exhibits characteristics similar to VSP data from more conventional sources. While the section is extremely ringy, the first breaks, as well as the upgoing and downgoing wavefields, are recognizable in the section. The ringy character observed in the correlated data is likely due to the quadratic scaling of the source signature. In other words, the ringiness is likely caused by the dependence of the source amplitude on ω^2. In Figure 11, the autocorrelation of the pilot trace is quite ringy, and this character is propagated into the correlated section.

To attempt to mitigate the ringy character of the correlated data, various deconvolution algorithms were tested, then applied to the VSP data. The pilot trace that was used for correlation was subjected to the following deconvolution algorithms: frequency domain spiking deconvolution, Weiner filtering, deterministic deconvolution (using both the pilot trace and the idealized synthetic sweep), and Gabor deconvolution (Figure 16).

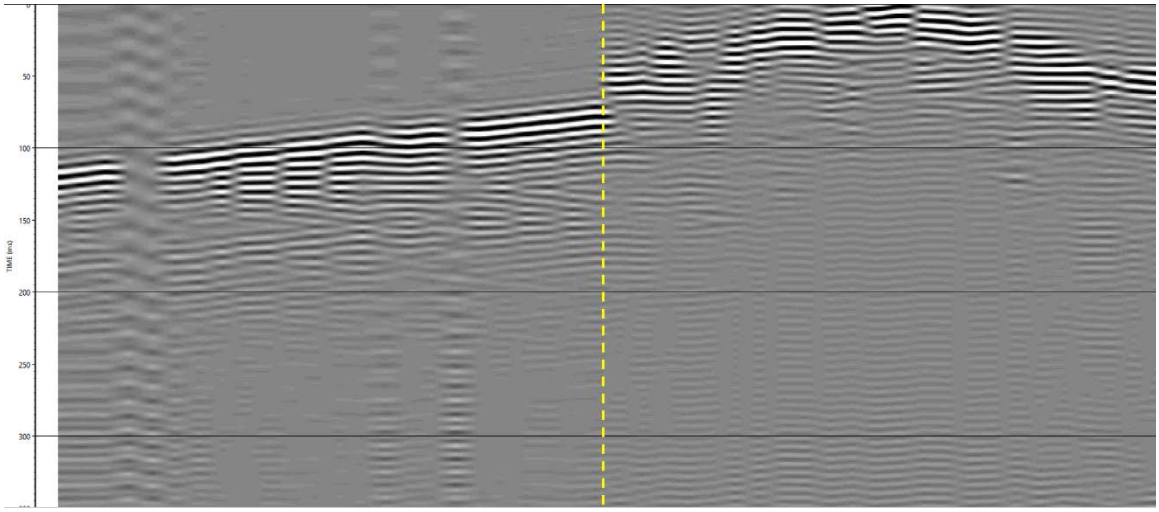

FIG. 14: Example of GPUSA borehole linear vibrator data using geophones in the geophysics well (left side) and a spread of geophones at the surface (right side). Source location is approximately in the centre of the surface spread. Data has been correlated with pilot trace. Sweep number 1026.

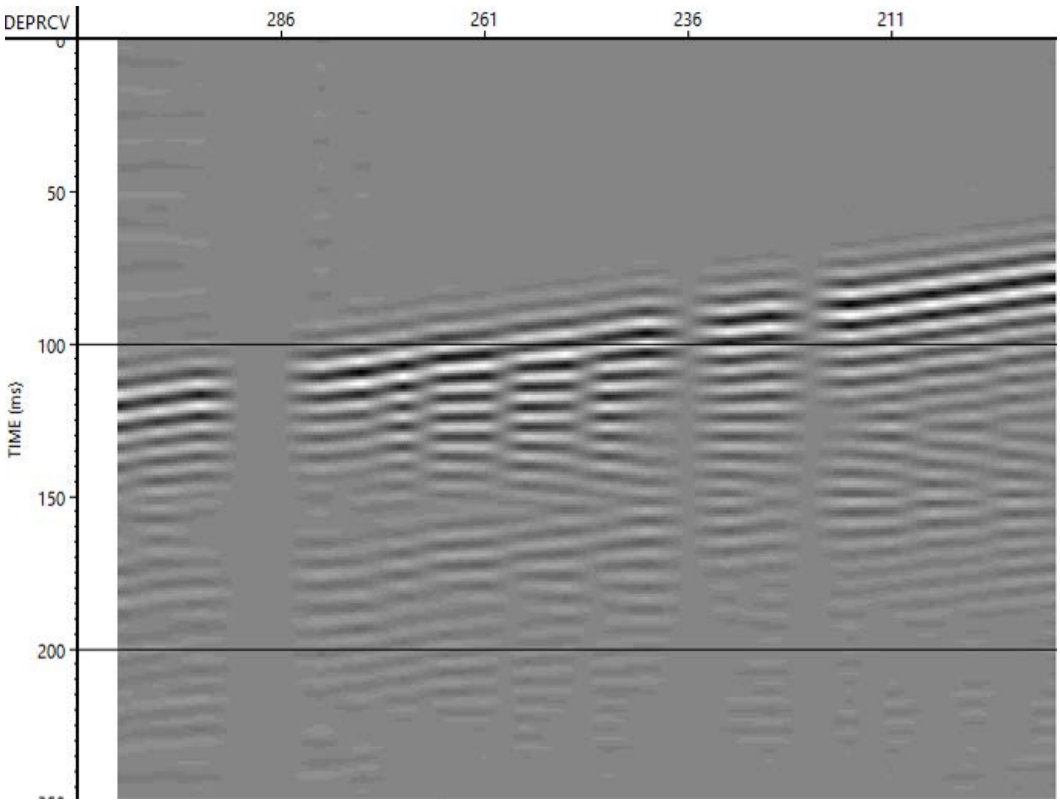

FIG. 15: VSP data from vertical component of multicomponent geophones in the geophysics well using GPUSA borehole linear vibrator as the source. Surface geophone pilot trace used for correlation. Data has been correlated with pilot trace. Sweep number 1026.

The spiking deconvolution and Weiner filtering algorithms perform quite poorly compared to the deterministic and Gabor deconvolution methods. Theoretically, the correlated trace in the left-most panel, used as a proxy for the source signature, should collapse to a delta spike, with maximum amplitude at $t = 0$. Deterministic deconvolution, whereby the spectrum of the input trace is multiplied by the inverse of the source spectrum, performs quite well when using both the pilot trace and the idealized synthetic sweep as the design trace. In both cases, low amplitude side lobes are observed. While both cases of deterministic deconvolution perform better than spiking deconvolution and Weiner filtering, Gabor deconvolution appears to outperform all other methods. The correlated trace has nearly collapsed to a perfect delta function, and minimal side lobes are observed.

The results of these tests indicate that applying Gabor deconvolution to the borehole linear vibrator data after correlation with the pilot trace will yield a dataset ready for further VSP data processing workflows. For each of the five permanent source tests, the recorded VSP data were correlated with the associated pilot trace, then a Gabor deconvolution algorithm was applied to the section. An example of the results of this process for sweep number 1026 is shown in Figure 17. Compared with Figure 15, the application of Gabor deconvolution generates encouraging results. In this figure, clear first breaks are visible, and the up-going and down-going wavefields can be identified easily. The ringy character observed in Figure 15 has largely been removed, and the resultant data are now ready for

further processing workflows. For comparison, a record from an Envirovibe located at the surface is shown in Figure 18.

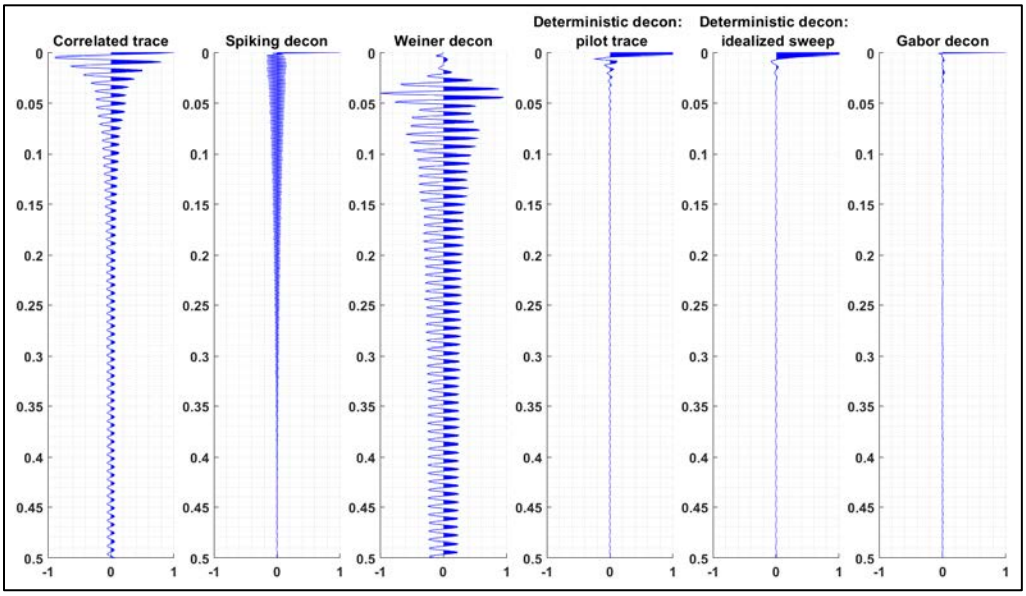

FIG. 16: Results of testing several deconvolution algorithms on correlated borehole linear vibrator data. Traces are (from left): correlated pilot trace; frequency domain spiking deconvolution result; Weiner filtering result; result of deterministic deconvolution with pilot trace; result of deterministic deconvolution with synthetic sweep; and Gabor deconvolution result. Sweep number 1026.

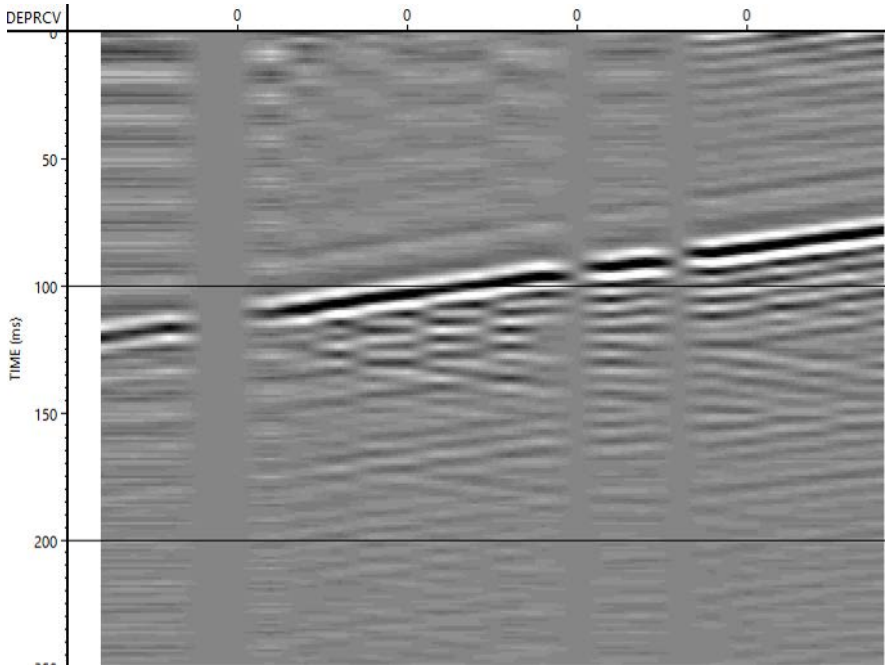

FIG. 17: VSP data from geophones in the geophysics well using the borehole linear vibrator as the source. Data has been correlated with the pilot trace and Gabor deconvolution applied. Sweep number 1026.

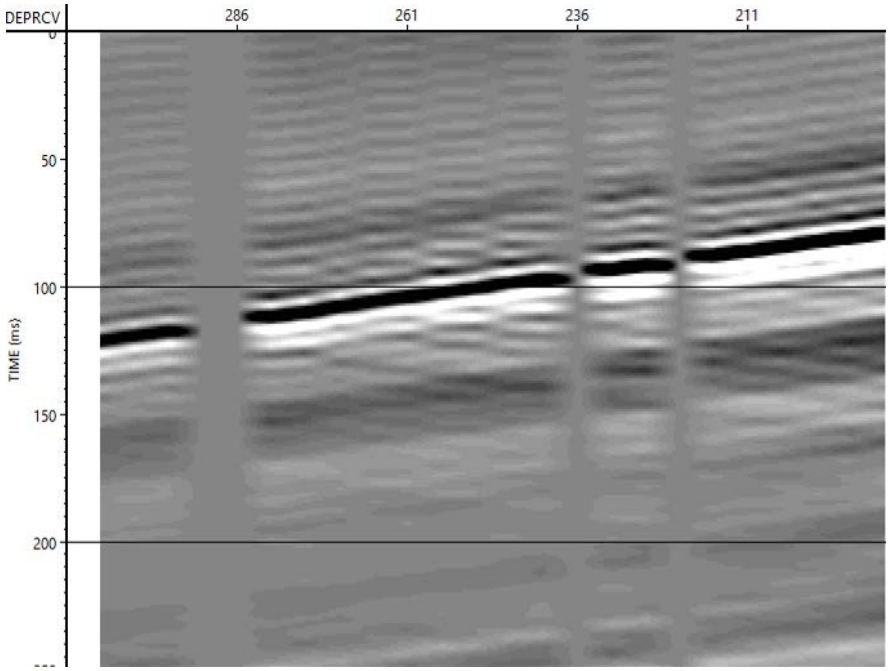

FIG. 18: VSP data from geophones in the geophysics well using a 10-150 Hz linear Envirovibe sweep. Gabor deconvolution applied to correlated data.

Compared with data acquired with the same receiver geometry and source-receiver offset, the borehole linear vibrator data is similar, if not superior, to data acquired using the conventional linear Envirovibe sweep over approximately the same bandwidth. The amplitude spectrum of the Vibroseis data (Figure 19) behaves as expected, with near-constant amplitude over the swept band of frequencies, and rapid decay of amplitudes outside this band. The amplitude spectrum of the borehole linear vibrator data (Figure 20) exhibits some expected characteristics; however it does raise a few questions.

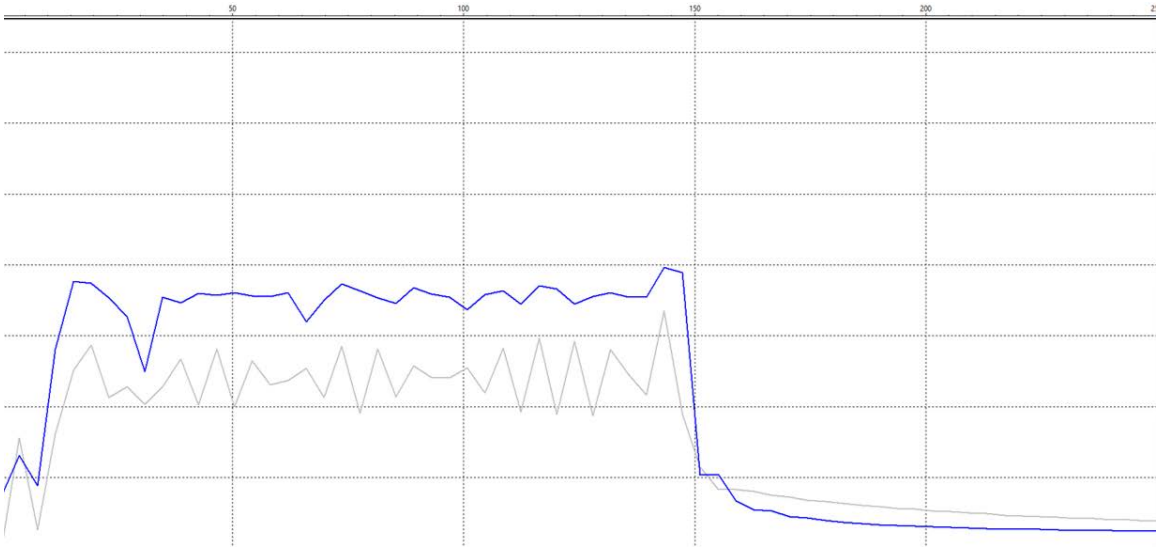

FIG. 19: Amplitude spectrum of VSP data acquired using a 10-150 Hz Envirovibe sweep. Average trace amplitude spectrum in blue.

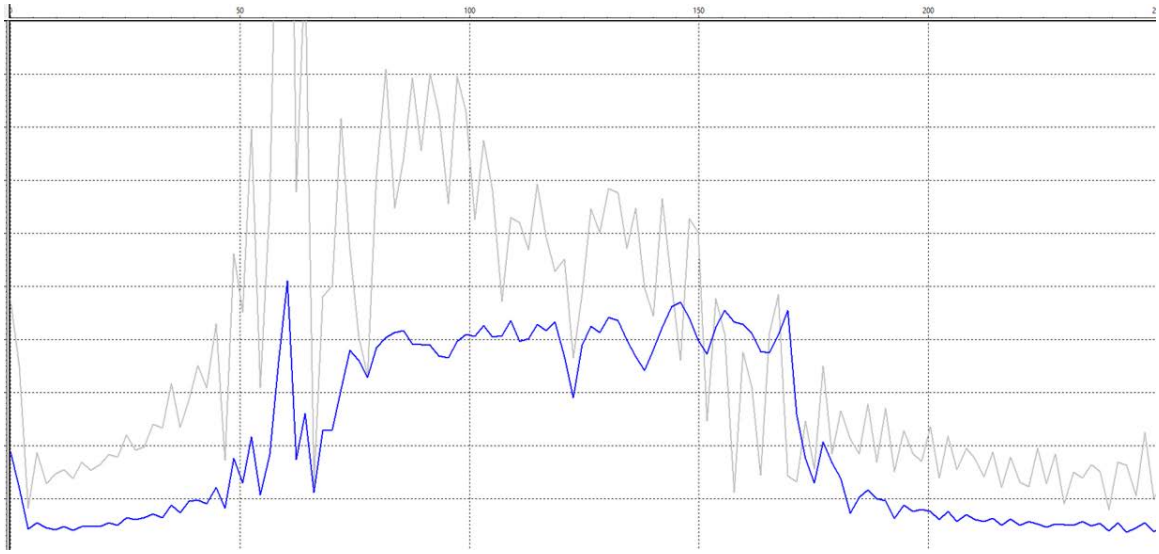

FIG. 20: Amplitude spectrum of VSP data acquired using GPUSA borehole linear vibrator sweep number 1026. Average trace amplitude spectrum in blue.

The spectrum of the borehole linear vibrator data increases approximately quadratically over the lower frequencies, then drops off rapidly at the maximum frequency of the sweep. The quadratic increase in amplitude is expected only in the pre-deconvolution spectrum due to the dependence of amplitude on ω^2; however, there still exists such an increase at lower frequencies in the post-deconvolution spectrum. There is also a slight spike in the amplitude at the lowest frequencies (approximately 0-4 Hz). Additionally, the spectrum does not increase quadratically to the maximum frequency (175 Hz), but rather to approximately 90-100 Hz before remaining relatively constant until the maximum frequency is reached. A third issue with the spectrum is that amplitudes are recorded at frequencies far beyond the maximum frequency of the sweep. While the Vibroseis data shows a steep decay to near-zero amplitude, the decay of borehole linear vibrator amplitudes is less rapid at high frequencies.

Similar VSP data processing workflows were applied to both the borehole linear vibrator and Envirovibe datasets. An overview of the general workflow is shown in Figure 21. Images of both of the datasets at various stages of the processing workflow can be seen in Figures 22-24. Gaps in the data in all of the images are noisy traces which were killed during the processing flow. The borehole linear vibrator data is single fold, as it was acquired using only one sweep; the Vibroseis data is 2-fold.

Figures 22 and 23 show the flattened upgoing recorded wavefield for each dataset, derived through flattening to first break times and median filtering. Figure 22 shows relatively clear reflected upgoing arrivals. The signal to noise ratio (SNR) could potentially be improved by using more than one sweep, thus increasing the fold. The same Gabor deconvolution algorithm was applied to each dataset before wavefield separation and appears to have negatively affected the Vibroseis data. Reflections are still readily identifiable in Figure 23; however the SNR appears to be lower than in Figure 22.

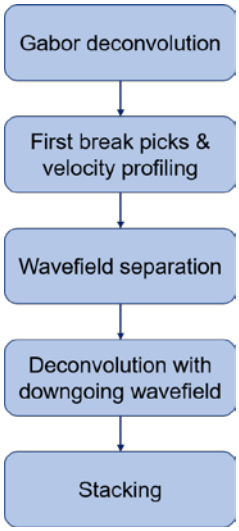

FIG. 21: General VSP data processing workflow for data acquired with both Vibroseis and borehole linear vibrator sources.

Figure 24 shows the final corridor stacks for both the borehole linear vibrator and Vibroseis datasets. The stacks were created by deconvolving the upgoing wavefield with the downgoing wavefield, removing residual downgoing energy with an F-K filter, and applying a 5-10/150-175 Ormsby bandpass filter. The corridor stacks are quite similar in character, and the same major reflectors are observed on both sections, with the injection interval, identified with arrows, located at approximately 250 ms. Both of the corridor stacks agree with synthetic seismograms that have been derived from well logs at the FRS, as well as other VSP datasets from the FRS (Figure 25, after Hall et al., 2018). The quality of the borehole linear vibrator corridor stack clearly shows that permanent seismic sources can be an extremely useful tool in geophysical monitoring.

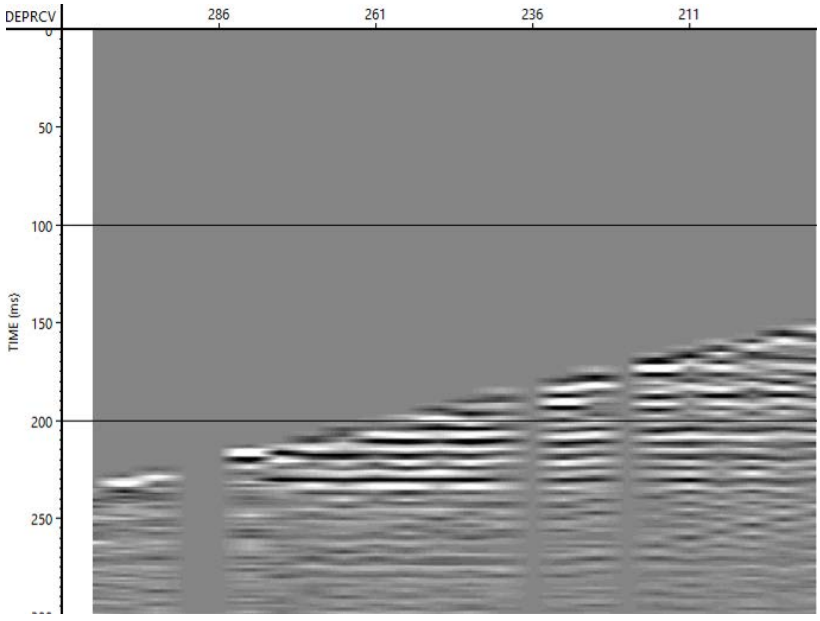

FIG. 22: Flattened upgoing wavefield for VSP data acquired using GPUSA borehole linear vibrator sweep number 1026.

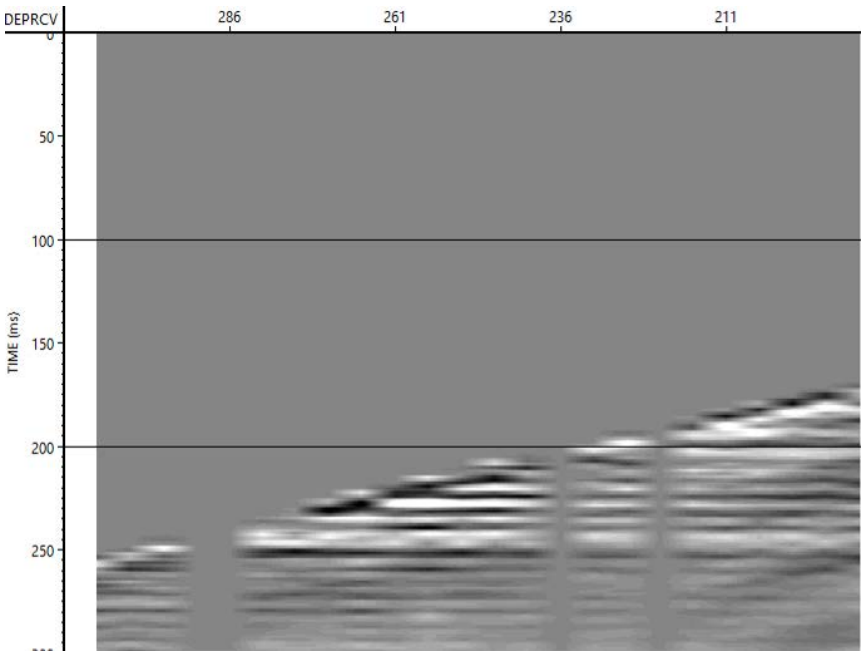

FIG. 23: Flattened upgoing wavefield for VSP data acquired using 10-150 Hz Vibroseis sweep.

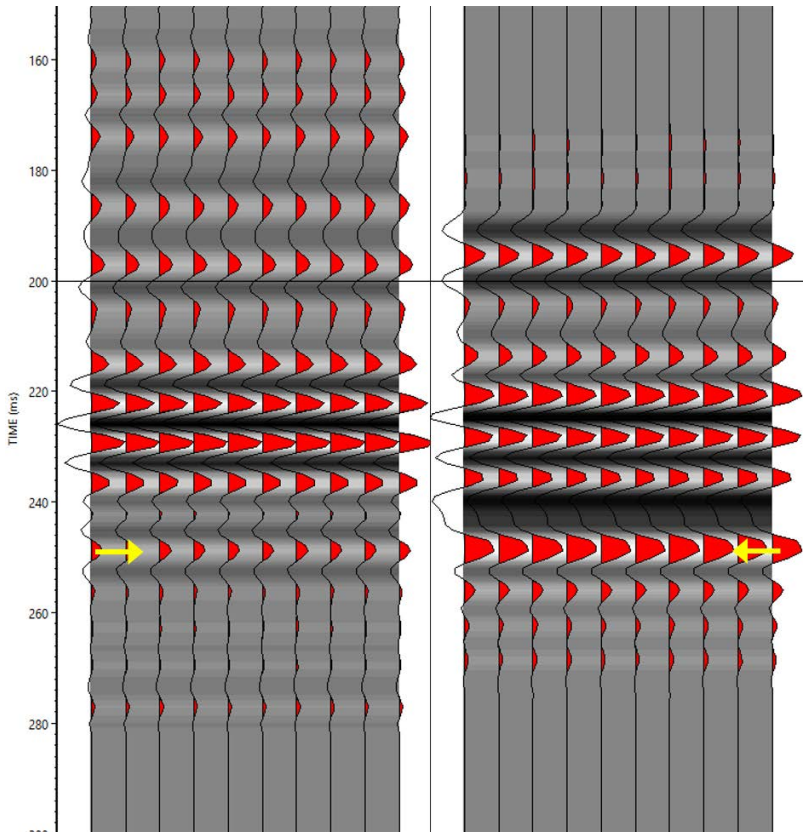

FIG. 24: Comparison of corridor stacks from VSP data acquired using GPUSA borehole linear vibrator sweep number 1026 (left) and 10-150 Hz Vibroseis sweep (right).

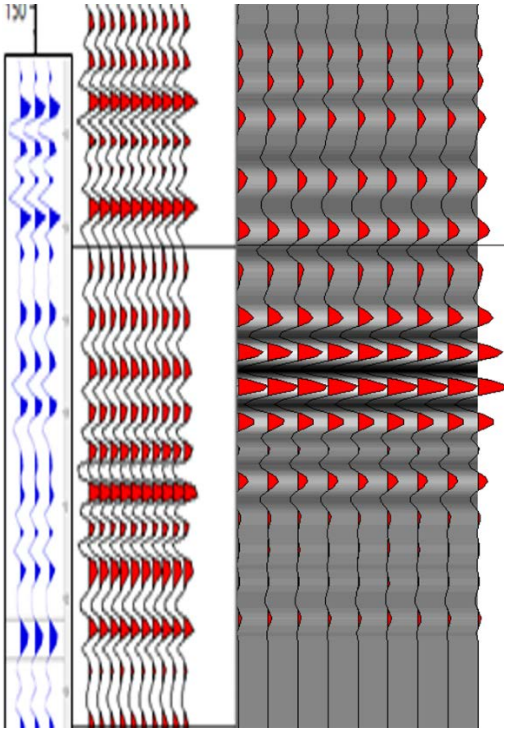

FIG. 25: Comparison of zero-offset synthetic seismogram (left), corridor stack from VectorSeis accelerometers and Inova Univibe source (1-150 Hz linear sweep, centre), and borehole linear vibrator corridor stack. (Modified from Hall et al., 2018).

CONCLUSIONS

Permanent seismic sources show promise as a tool for acquiring time lapse seismic datasets. In this study, the acquisition parameters for the testing of permanent sources were described, with particular emphasis on the initial tests of the GPUSA borehole linear vibrator. In the absence of source accelerometer recordings, data acquired with this source may be correlated with a pilot geophone trace to produce usable sections for further processing. However, this correlated data is quite ringy in character. Gabor deconvolution was found to generally mitigate this problem. Applying a conventional VSP data processing workflow to the borehole linear vibrator data yields corridor stacks that are superior to the corridor stacks from Vibroseis datasets and encourages the further use of this permanent buried seismic source as a geophysical monitoring tool.

FUTURE WORK

Going forward with the testing of the GPUSA permanent sources and the analysis of the recorded data, there are several potential avenues for further investigations. To improve the SNR and the image quality of the borehole linear vibrator data, the fold of the data should be increased by stacking data from several sweeps. Additionally, to attempt to mitigate the ringy character of surface linear vibrator data, a new type of steel pile will be installed and tested in the near future. As this study focused primarily on VSP data, future work should also move towards processing surface geophone data from the borehole linear vibrator, as well as processing surface and VSP data acquired using a surface linear

vibrator. This may be aided by installing additional steel piles, allowing for more source locations.

ACKNOWLEDGEMENTS

We are grateful to the sponsors of CREWES and of the CaMI.FRS JIP, the University of Calgary through the Canada First Research Excellence Fund (CFREF), and NSERC through grant CRDPJ 461179-13 for financial support. We also wish to acknowledge Howard Wilkinson of GPUSA for his role for providing the linear vibrators and assisting with installation, testing, and training on these devices.

REFERENCES

Daley, T. M., and Cox, D, 2001, Orbital vibrator seismic source for simultaneous P- and S-wave crosswell acquisition: Geophysics, **66**, 1471-1480.

Hall, K.H., Bertram, K.L., Bertram, M., Innanen, K., and Lawton, D.C., 2018, CREWES 2018 multi-azimuth walk-away VSP field experiment: CREWES Research Report, **30**, this volume.

Isaac, J.H., and Lawton, D.C., 2014a, Preparing for experimental CO_2 injection: Geology of the site: CREWES Research Report, **26**, 42.1-42.9.

Spackman, T.W., and Lawton, D.C., 2017, Seismic monitoring with continuous seismic sources: CREWES Research Report, **29**, 68.1-68.12.